IEEE Photonics Journal
An IEEE Photonics Society Publication

Open Access

Ultrahigh Resolution Optical Reflectometry Based on Linear Optical Sampling Technique With Digital Dispersion Compensation

Volume 9, Number 6, December 2017

Shuai Wang
Xinyu Fan
Zuyuan He

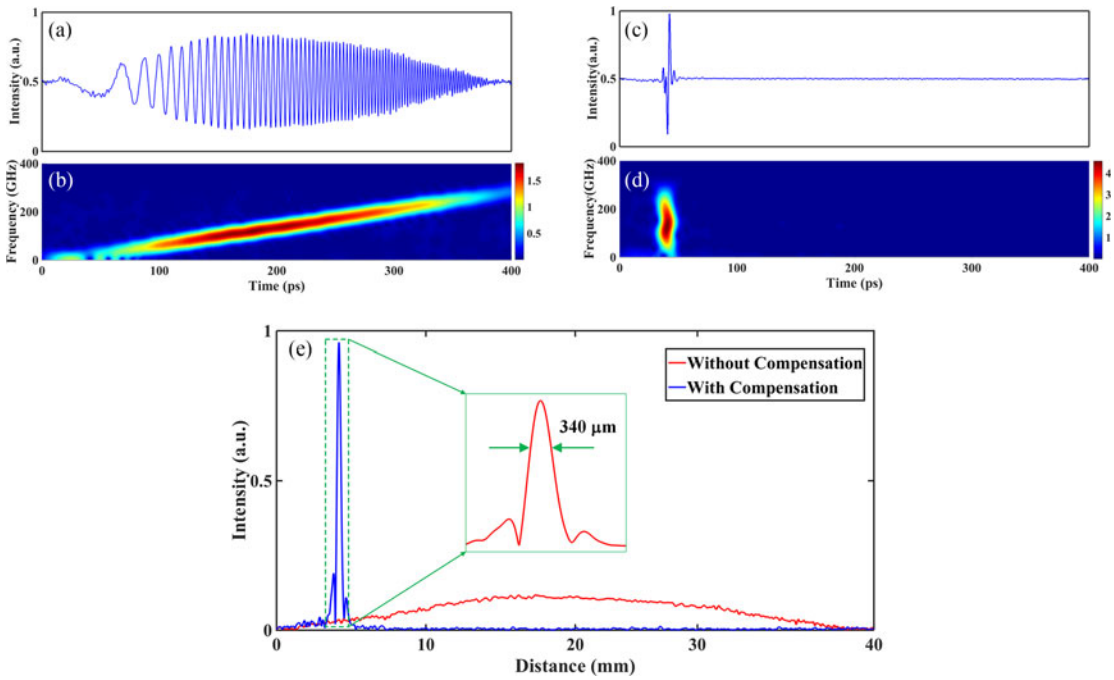

DOI: 10.1109/JPHOT.2017.2762352
1943-0655

IEEE photonics SOCIETY

IEEE

Ultrahigh Resolution Optical Reflectometry Based on Linear Optical Sampling Technique With Digital Dispersion Compensation

Shuai Wang,[1] **Xinyu Fan**,[1] **and Zuyuan He** [1]

[1]Shanghai Institute for Advanced Communication and Data Science, State Key Laboratory of Advanced Optical Communication Systems and Networks, Shanghai Jiao Tong University, Shanghai 200240, China

DOI:10.1109/JPHOT.2017.2762352

Manuscript received September 2, 2017; revised September 22, 2017; accepted October 9, 2017. Date of publication October 11, 2017; date of current version October 30, 2017. This work was supported by the National Natural Science Foundation of China under Grant 61775132, Grant 61327812, and Grant 61735015. Corresponding author: Xinyu Fan (e-mail: fan.xinyu@sjtu.edu.cn).

Abstract: We demonstrate an ultrahigh-resolution optical time domain reflectometry (OTDR) system by using a mode-locked laser as the pulse source and a linear optical sampling technique to detect the reflected signals. Taking advantage of the ultrashort input pulse, the large detection-bandwidth, as well as the low timing jitter of linear optical sampling system, a sub-mm spatial resolution is achieved. As the pulse-width is broadened with the increase of distance due to chromatic dispersion and large bandwidth of the ultrashort pulse, by adopting digital chromatic dispersion compensation, we achieved a spatial resolution of 340 μm when measuring the reflector at 10 km. This technique helps OTDR find new foreground in long-range and ultrahigh-resolution distributed applications such as remote optical identification device detection for diagnosing passive optical network links, or precisely detecting fault positions in aircrafts.

Index Terms: Optical reflectometry, linear optical sampling, chromatic dispersion compensation.

1. Introduction

Distributed fiber sensing technologies have been used to characterize optical links via backscattered signals. For some high-end applications such as the structural health monitoring of aircrafts [1], and the reading technique of optical identification (OID) devices which use spatially multiplexed fiber Bragg gratings (FBGs) inside fiber connectors as "0" and "1" for access network management [2], it is of great significance to precisely locate the reflections with a very strict requirement for high spatial resolution. Especially for aircrafts, it is necessary to monitor the optical fiber inside the aircraft with a spatial resolution of better than 1 mm over several hundred meters. The two most well-known long-range distributed sensing technologies are optical time domain reflectometry (OTDR) and optical frequency domain reflectometry (OFDR). However, the spatial resolution of commercial OTDR systems is limited to $\sim$0.3 m because a narrower pulse requires a detector with faster response and larger detection-bandwidth [3]. Thanks to the ultra-high-sensitivity of single-photon detectors and the photon counting technology, photon-counting OTDR (ν-OTDR) [4]–[7] has drawn an intense attention with a much improved spatial resolution to $\sim$1 cm. However, the

spatial resolution is finally limited by the timing jitter of the photon-counting detector (the state-of-the-art timing jitter is ∼40 ps) [8]. OFDR faces the similar situation, and its spatial resolution is determined by the frequency tuning span and its measurement range is restricted by the coherence length of the optical source. However, an ultra-high spatial resolution with a long measurement range is unattainable because of the difficulty in achieving a high coherent optical source with a wide frequency tuning span, together with a fine sweep linearity simultaneously [9], [10]. In other words, there is a tradeoff between the measurement distance and the spatial resolution. Recently, an alternative method to mitigate the phase noise by increasing the frequency sweeping rate is proposed, however the spatial resolution is still restricted by the detection bandwidth [11], [12].

To break the limitations of achieving an ultra-high spatial resolution together with a long measurement range, it is necessary to find a technique with a large detection-bandwidth. Linear optical sampling (LOS) technique [13]–[15], known for the capability of observing the complex amplitude response of ultrashort optical pulses using slow electronics with a low bandwidth, and its shot-noise limited sensitivity, has been used in many fields for monitoring the waveform in high speed transmission systems. The signal under detection (SUT) interferes with the sampling signal launched from the mode-locked laser (MLL) and is then detected by the ordinary photo-detectors. Because the timing jitter of the MLL is several femtoseconds, the sampling rate can be up to 100 TS/s, and this makes it possible to measure ultrashort pulse launched from pulsed lasers and its reflected lightwave from optical fibers. In addition, MLLs usually have a linewidth better than 1 kHz, which makes it a promising optical source for long-range sensing applications. Therefore, the adoption of LOS technique in reflectometry system has the potential to realize an ultra-high spatial resolution with a long measurement range.

We present here a novel ultra-high-resolution OTDR technique, in which an MLL is used as the pulse source launching ultrashort pulses, and a LOS system is used to measure the signals. Thanks to the ultrashort pulse-width of optical source and the large detection bandwidth of LOS system, the theoretical spatial resolution of sub-mm is achieved. Moreover, the low phase noise of MLL allows the measurement distance be up to tens of kilometers. By using this technique, we realized a 340 μm spatial resolution when measuring the reflector at 10 km with proper digital chromatic dispersion (CD) compensation, which exhibits a better spatial resolution with enhancement factor of 1000 compared to conventional OTDR and 30 compared to ν-OTDR. To the best of our knowledge, it is the highest spatial resolution have ever been achieved at such a distance. This paper was presented in part in [16]. Section 2 describes the measurement principle of linear optical sampling technique used for reflectometry. The experimental demonstrations of proposed technique are given in Section 3. Section 4 explains the digital chromatic dispersion compensation process. The influence of the phase noise caused by carrier frequency and repetition rate fluctuation is discussed in Section 5, and Section 6 summarizes the paper.

2. Principle of Experiment

The schematic for the experimental setup is shown in Fig. 1. For the ultra-high-resolution OTDR system, an MLL is acting as a pulse generator. The ultrashort pulses are launched through the circulator into the fiber under test (FUT) and backscattered to the third port of the circulator. To characterize the backscattered signal, we utilize another MLL as the sampling laser.

The ultrashort pulses from the MLL have a comb-like spectrum, and the electric field of the signal to be measured in the LOS system can be expressed as

$$E_s(t) = \sum_m C_m \, exp\,\{j\,[(\omega_S + m\Omega_S)\,t]\} \tag{1}$$

and the envelope of the signal is

$$I\,(t) = \sum_m C_m \, exp\,\{jm\Omega_S t\} \tag{2}$$

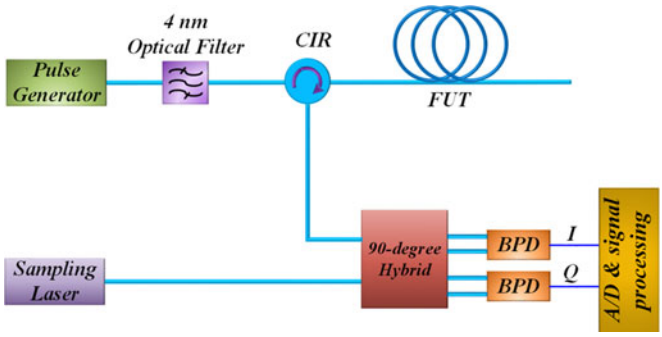

Fig. 1. Experimental setup of OTDR system based on linear optical sampling technique. CIR, optical circulator; FUT, fiber under test; BPD, balanced photodetector.

where C_m is the amplitude of comb tooth, ω_S is the carrier frequency, and $\Omega_S = 2\pi f_S$(f_S is the repetition rate). The electrical field of the local sampling pulse which comes from another MLL is given by

$$E_L(t) = \sum_n C \exp\{j[(\omega_L + n\Omega_L)t]\} \tag{3}$$

where ω_L is the carrier frequency and $\Omega_L = 2\pi f_L$ (f_L is the repetition rate). Assuming the local sampling source has a rectangular-shaped spectrum in the frequency range, and the amplitude of each comb tooth is a constant C. The sampling pulses interfere with the SUT in the 90 degree hybrid, and the electric field of the total lightwave is given by

$$E_{total}(t) = E_S(t) + E_L(t) \tag{4}$$

Assuming $R(t)$ is the impulse response of the slow photodetector, the output signal of the detector becomes

$$\begin{aligned} S(t) &= \int E_{total}(\tau) \cdot E^*_{total}(\tau) \cdot R(t-\tau)\, d\tau \\ &= \int [E_S(\tau) \cdot E^*_S(\tau) + E_L(\tau) \cdot E^*_S(\tau) + E_S(\tau) \cdot E^*_L(\tau) + E_L(\tau) \cdot E^*_L(\tau)] R(t-\tau)\, d\tau \end{aligned} \tag{5}$$

where the first and last products are self-product terms and the second and third ones are cross-product terms. With a much smaller bandwidth compared with the short pulse, the output of the photodetector becomes its impulse response. For the sampling process, when the time-independent difference of the two lasers meet the relationship: $\Delta\Omega = \Omega_S - \Omega_L << \Omega_S$ *or* Ω_L, the impulse response of the photodetector is regarded as a low pass filter with smaller bandwidth than the repetition rates of both lasers, and the impulse response $R(t-\tau)$ is much shorter than the final result, (5) becomes

$$\begin{aligned} S(t) &= 2\int \left\{ \sum_l \sum_k C C_l \exp\{j[(\omega_S + l\Omega_S)\tau]\} \exp\{j[-(\omega_L + k\Omega_L)\tau]\} \right\} R(t-\tau)\, d\tau \\ &= 2\int \left\{ \exp[j(\omega_S - \omega_L)\tau] \sum_m C_m \exp\{jm\Delta\Omega\tau\} \right\} R(t-\tau) d\tau \\ &= 2\exp[j(\omega_S - \omega_L)t]\, I'(t) \end{aligned} \tag{6}$$

where $I'(t) = \sum_m C_m \exp\{jm\Delta\Omega t\}$.

From (6) we can derive that the final envelope of the SUT can be recovered with a bandwidth compression ratio of $\Omega_S/\Delta\Omega$, while the carrier frequency is determined by the differential carrier frequency of the two optical sources. For the special case when the carrier frequencies of the

two optical sources are locked, which may be expressed as $\omega_S - \omega_L = 0$, the exact envelope and phase term of the SUT are obtained. The update rate of the sampling process is then determined to be $\Delta\Omega/2\pi$. There is no requirement for the linewidth and carrier frequency stability of the two lasers when only measuring the signal intensity. To obtain the whole information of the signal, the sampling pulses must completely cover the data signal in the spectrum domain [15]. It is worth noting that the flat spectrum of the sampling pulses is essential to avoid the sampling distortion in signal reconstruction applications. This condition is maintained in experiment by using an MLL with smooth optical spectrum.

Apart from the detection method using LOS technique, the other implementation of this ultra-high spatial resolution OTDR system is quite similar to the conventional coherent OTDR system.

3. Experiments

In this ultra-high-resolution OTDR system, ultrashort optical pulses with a central wavelength of 1550 nm from an MLL are launched into the FUT through a circulator. The reflected signal is coupled into the third port of the circulator, interfering with the pulses coming from the sampling MLL at the optical 90-degree hybrid and then detected by a pair of 150-MHz balanced photo-detectors (BPDs) (Thorlabs PDB450C). The signals are sampled by a 14-bit analog-to-digital card (ADC) and collected with a personal computer. The two MLLs used in this experiment are free-running lasers with timing jitter of about 60 fs. The duration time of the pulses launched from the sampling laser is less than 100 fs, which means the spatial resolution limitation of the OTDR system is 10 μm ignoring the CD effects and nonlinear effects.

At the first experiment, we make a measurement for a short distance by comparing this technique with the optical low coherence reflectometry (OLCR). We prepared a 1.6 cm polarization maintained FBG (PM-FBG) for testing. The reflected signal was received by a polarization diversity scheme both in LOS-based OTDR (LOS-OTDR) and OLCR. The sampling laser has a repetition rate of 50 MHz, and the peak power of the probing pulse is about 100 mW. We adjust the repetition rates of the pulse generator to be 250.001 MHz, and the equivalent sampling rate of LOS-OTDR system is 25 TS/s when the real sampling rate of the ADC is 100 MHz, which is very fast for us to clearly observe the pulses.

As for the OLCR system, the accuracy of step motor is set as 4 μm. The measured traces of p- and s-polarizations of the reflected signals are shown in Fig. 2. The beat length of the PM-FBG is measured to be $\sim$2 mm both by LOS-OTDR (shown in Fig. 2(a)) in 10 ms and OLCR in 30 min (shown in Fig. 2(b)), and we can clearly see the interference pattern inside the grating due to the high spatial resolution. Affected by the environmental vibrations, the traces measured by OLCR show more distorted interference pattern than that of LOS-OTDR due to the longer maesurement time.

We also make a measurement for a long distance, and we use an active MLL (Pritel UOC) with a changeable repetition rate and 6 ps pulse duration time as the pulse source in the experiment. The peak power of the delivered pulses is 330 mW. Since the repetition rate of the optical pulse generator is about 500 MHz, the sampling window is $Ts = 2$ ns, corresponding to a 20 cm measurement range. To locate the reflection events beyond this measurement range, it is necessary to set a reference position (the reference reflector in this experiment is the weak reflector of the connection point between the circulator and the FUT) shown in Fig. 3(a). Assuming that at time t_0, the pulse reflected from the reference reflector is the *N -th* pulse and the pulse reflected from the point to be located is the *M -th* pulse, the distance between the reference reflector and the located point can be expressed as

$$\Delta L = \Delta z + cT_d |M - N| / n \tag{7}$$

where Δz is the distance shown in the sampling window, c is the speed of light and n is the refractive index. If we change the repetition rate, $1/T_d$ of the optical pulse generator, Δz changes and $|M - N|$ can be calculated. Therefore, the position of the reflection can be exactly located.

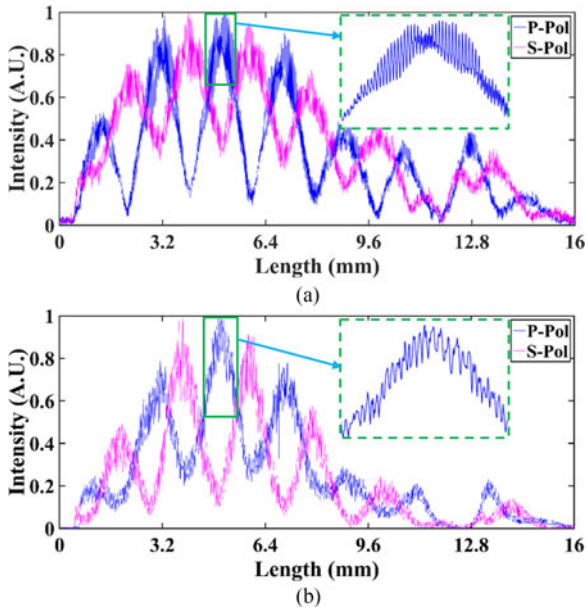

Fig. 2. Beat length measurement of PM-FBG by using (a) LOS-OTDR and (b) OLCR.

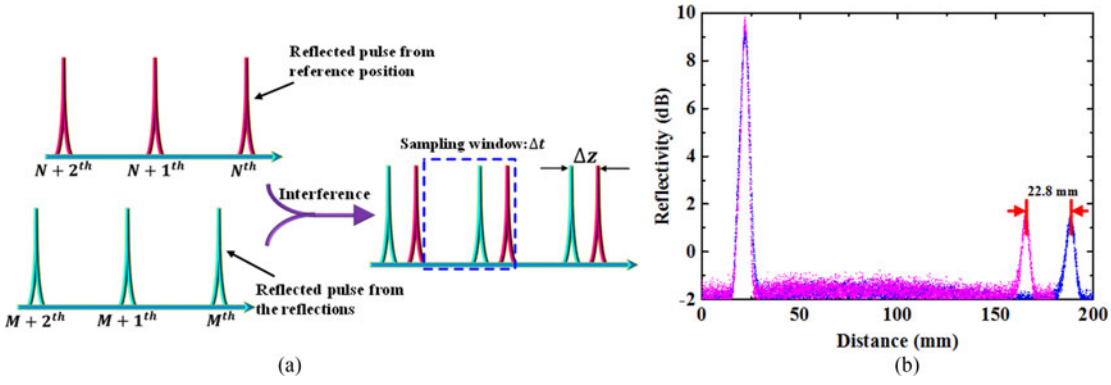

Fig. 3. (a) Principle of locating the reflection events. (b) Proof-of-concept experimental results of a 900-m SMF in one sampling window.

The proof-of-concept measurement of a 900-m SMF is depicted in Fig. 3(b). In the experiment, we choose the position of APC-APC connector between the circulator and FUT as the reference position. Two lines in the window (red and blue) show two peaks from the reference position and from the position to be located with two different repetition rates of the optical pulse generator. When the repetition rate is $1/T_{d1} = 500.0125$ MHz, the distance shown in the sampling window between the two peaks is $\Delta z_1 = 143.42$ mm as shown by the red line. The blue line shows the two peaks when the repetition rate is $1/T_{d2} = 500.0250$ MHz, and the distance shown in the sampling window between them is $\Delta z_2 = 166.22$ mm. By using (7), we calculated that the position of the peak is 912.021 m from the reference reflector. Note when the reflection is very close to the reference reflector, the repetition rate is required to be much changed for distinguishing the two peaks. Meanwhile, the repetition rate of the sampling laser should also be changed to keep high sampling rate according to (4).

Another solution to locate the reflection events without this adjustment is to make a long sampling window by decreasing the repetition rate of the sampling laser using pulse-selecting technique. For example, if we decrease the repetition rate to 10 kHz, the corresponding detection distance would be increased to 10 km.

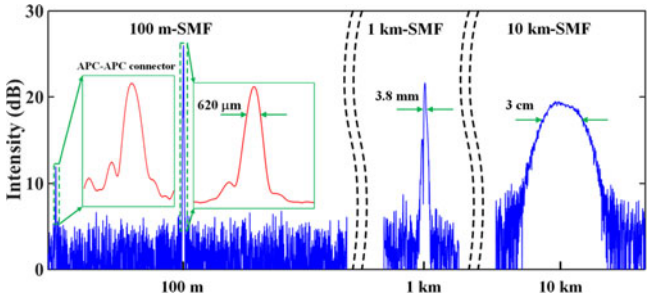

Fig. 4. Spatial resolution achieved at different distances.

To test the spatial resolution at different distances, we set the FUT to be a 100-m SMF, a 1-km SMF and a 10-km SMF, respectively, all fabricated by Yangze optical fiber and cables company (YOFC). As shown in Fig. 4, we may find that the full width half maximum (FWHM) of the reflection peak at 100 m is 620 μm, which is slightly broadened from the original pulse coming from the laser. As the pulse propagates to the end of the SMF at 1 km, the reflection peak is broadened to 38 ps, which corresponds to a spatial resolution of 3.8 mm. The spatial resolution becomes 3 cm after passing through the 10 km SMF. The pulse extinction ratio, which defined as the ratio between the amplitude of the main peaks to the amplitude of the sidelobes, is 54 dB, while the effective number of bits (ENOB) of the ADC is about 11 bits (equivalent to 66 dB dynamic range), and the shot noise is below the sidelobes of the probe pulses. The single shot dynamic range of the LOS system is therefore limited by the pulse extinction ratio to be 54 dB. If we define the reflectivity of the Fresnel peak from a FC/PC connector to be -14 dB, then the sensitivity is -68 dB. However, we still notice that we cannot observe the Rayleigh backscattered signal since the reflectivity of Rayleigh backscattered signal is -100 dB for a spatial resolution of 1 mm, which is below the noise floor. We believe that the pulse broadening is mainly caused by CD effect as it propagates in the FUT and this has been predicted in [17]. As the spatial resolution increases, it is necessary to deal with the influence of dispersion which depends on the wavelength range of the probe pulses and the measurement distance. To make this process clear, the influences of chromatic dispersion on spatial resolution are discussed in the following Section.

4. Digital First-Order Chromatic Dispersion Compensation

The electrical field of a Gaussian pulse can be expressed as

$$E\,(0,\,t) = A\,(t)\;exp\,\left(-\alpha t^2 + j\omega_0 t\right) \tag{8}$$

where $A(t)$ is the pulse amplitude and $\alpha = (2\sqrt{ln2}/\tau_p^2)/2$ (τ_p is the pulse duration time). As the ultrashort optical pulse propagates through the single mode fiber, it experiences the dispersion and the electrical field becomes

$$E\,(z,\,t) = A'\,(t)\left(\alpha^2+\beta^2\right)^{-1/4} exp\left[-\alpha\beta^2\left(\alpha^2+\beta^2\right)^{-1}t^2\right]\;exp\left\{-j\omega_0 t - j\alpha^2\beta\left(\alpha^2+\beta^2\right)^{-1}t^2\right\} \tag{9}$$

where $\beta = \pi c/(D\,z\lambda_0^2)$, D is the dispersion coefficient, λ_0 is the center wavelength of the ultrashort optical pulse, and z is the propagation distance from the pulse source. Then the pulse duration time can be written as

$$T\,(z) = T_p\sqrt{1+\left(\frac{1.47D\,z{\lambda_0}^2}{{T_p}^2}\right)^2} \tag{10}$$

Since the main limitation of spatial resolution at long distance is CD effect, we believe that a better resolution may be achieved if CD effect is properly compensated. DCF compensation technique or mid-link optical phase conjugation (ML-PC) technique [18] are well-known conventional techniques

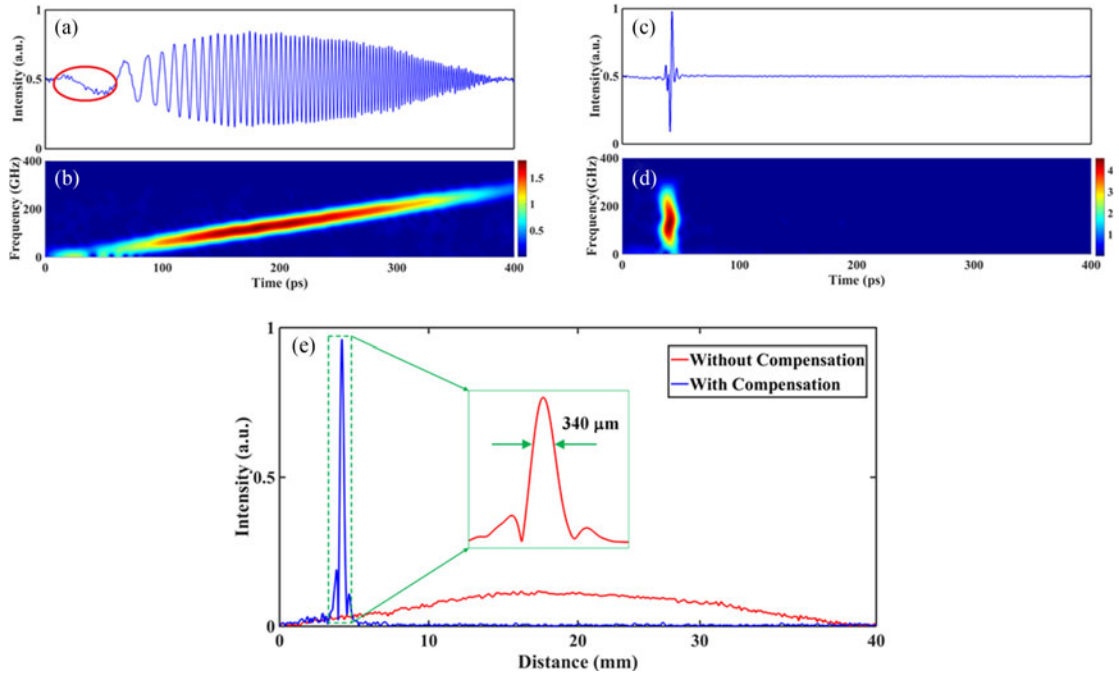

Fig. 5. (a) Reflection peak without CD compensation; (b) Time-frequency map of the reflection peak without CD compensation; (c) Reflection peak with CD compensation; (d) Time-frequency map of the reflection peak with CD; (e) Details of the reflection peak at 10 km with/without CD compensation.

for dispersion compensation, but it is impractical for optical fiber sensing system since they require the transmission link to be modified, which significantly reduced the flexibility of the system. Aa a well-known technique used in the optical communications systems [18], the digital chromatic dispersion compensation method is chosen in this experiment. Comparing (8) with (9), the response function of CD effect in SMF in frequency domain is

$$H_f(\omega) = exp\left[j\left(\frac{1}{2}\right)\beta z(\omega - \omega_0)^2\right] \tag{11}$$

Since LOS technique has the capability to obtain both intensity and phase information of the signal, digital compensation in the frequency domain would be a good option to mitigate the degrading effects caused by CD effect. For CD compensation in the experiment, the second pulse source used is a passive MLL (Menlo Systems) with a much shorter pulse duration time of 100 fs with the output power of 100 mW. In order to suppress the SNR degradation caused by nonlinear distortions, the pulses are filtered using a 4 nm optical bandpass filter and the pulse duration time is broadened to be 2 ps with an average power of 2 mW. To maintain the accuracy of extracted phase information, we choose a reflector at 10 km with a moderate SNR to make compensation. According to (11), the CD effects impose a quadratic phase modulation to the ultrashort pulses in the frequency domain, and the local angular frequency has to be changed linearly accordingly. This has been verified when measuring reflectors at 10 km as shown in Fig. 5. The pulses are broadened to be about 300 ps shown in Fig. 5(a) and the time-frequency map shown in Fig. 5(b) illustrates that the pulses become linearly chirped, which agrees well with the analysis above. Therefore, the compensated reflections can be written as

$$E'(z, t) = F^{-1}\left\{F\left[E(z, t)\right]H_f^*(\omega)\right\} \tag{12}$$

where F and F^{-1} means Fourier transform and inverse Fourier transform.

The 10-km SMF from YOFC in this experiment has a dispersion coefficient $D = 17$ ps/(nm•km) when the central wavelength is 1550 nm. After determining an approximate distance L of the

reflector by using the location method mentioned in Session 3, we chose the chromatic dispersion coefficient to be DL, then the reflector is compensated according to (12). The information of the compensated reflector is shown in Fig. 5(c) and (d). The time domain signals in Fig. 5(c) and time-frequency map in Fig. 5(d) show that the pulse is compressed and the linear chirp disappears. After the digital CD compensation, the pulse is compressed to 3.4 ps, which corresponds to a spatial resolution of 340 μm, as shown in Fig. 5(e).

5. Discussions

In OTDR systems, the achievement of a higher spatial resolution requires shorter pulses to be launched, which bears more CD effects since shorter pulses have larger wavelength range. Moreover, shorter pulses means higher peak power for the same averaged power, and in some other experiments we find that when launching probe pulses with higher peak power, nonlinear effects cannot be ignored. In that case, the reflected power degrades and a worse spatial resolution was achieved. Since the nonlinear effects exhibit an opposite influence to the CD effects in SMF, the total influence cannot be compensated completely. The nonlinear effects can be the dominant restrictions for further improvement in the spatial resolution after the digital CD compensation. As we mentioned before, we still cannot observe the Rayleigh backscattered signals since the noise floor is still about 30 dB above the signals. Since the sensitivity of LOS technique is nearly shot-noise limited, for some applications which requires to observe the Rayleigh backscattered signals, it is necessary to average the multiple traces.

All experiments shown in this paper are based on two free-running MLLs without phase-locking electronics. For a fully self-referenced MLL, the carrier frequency and the repetition rate are stabilized and locked to a reference atom clock. However the carrier frequency and repetition rate of MLLs in these experiments are not locked to each other. The carrier frequency phase noise and the repetition rate phase noise can be represented as $\phi_c(t)$ and $\phi_r(t)$ respectively. Therefore the reflected signals measured in this experiment can be expressed as

$$S'(t) = 2\,exp\,\{j\,[(\omega_S - \omega_L)\,t + \phi_c\,(t)]\} \sum_m C_m\,exp\,\{j\,[m\Delta\Omega t + m\phi_r\,(t)]\} \tag{13}$$

The carrier frequency phase noise may be classified to the phase noise which reflects the linewidth and the carrier frequency fluctuations, and in this sampling process it can be expressed as

$$\phi_c\,(t) = \phi_{Sc}\,(t) - \phi_{L\,c}\,(t) \tag{14}$$

where $\phi_{Sc}(t)$ is the carrier frequency noise of signal laser and $\phi_{L\,c}(t)$ is the carrier frequency noise of sampling laser. The repetition rate phase noise, which results in the timing jitter in the time domain, can be converted as the pulse envelope's temporal deviation of the optical pulse train from perfect periodic temporal positions. We express the repetition rate phase noise as

$$\phi_r\,(t) = N\phi_{Sr}\,(t) - \phi_{L\,r}\,(t) \tag{15}$$

where N is an integer equals to the ratio of the repetition rates of these two lasers. Similar to the discussion in Section 2, from (13) we may find that the repetition rate phase noise will cause more sampling distortions when generating shorter pulses, while the carrier frequency phase noise does not play any roles in the measurement of the envelope of the backscattered signals. In this experiment, since we characterize the complex signals, both the carrier frequency phase noise and the repetition rate phase noise cannot be neglected. Therefore, we set up an experiment to evaluate those noise as shown in Fig. 6. As we noticed that the carrier frequency noise is a fast-changing parameter, for the sake of intuitiveness, the carrier frequency fluctuation, which is the differential of carrier frequency phase, $d\phi_c(t)/dt$, is shown in Fig. 6(b). The repetition rate phase noise $\phi_r(t)$ is a slow-changing parameter, and is obtained in Fig. 6(c) for comparison. In this 1 ms measurement period, the carrier frequency fluctuation is about 200 kHz, which means the coherent time is much longer than the sampling period. As for the experimental results, the phase fluctuations illustrated

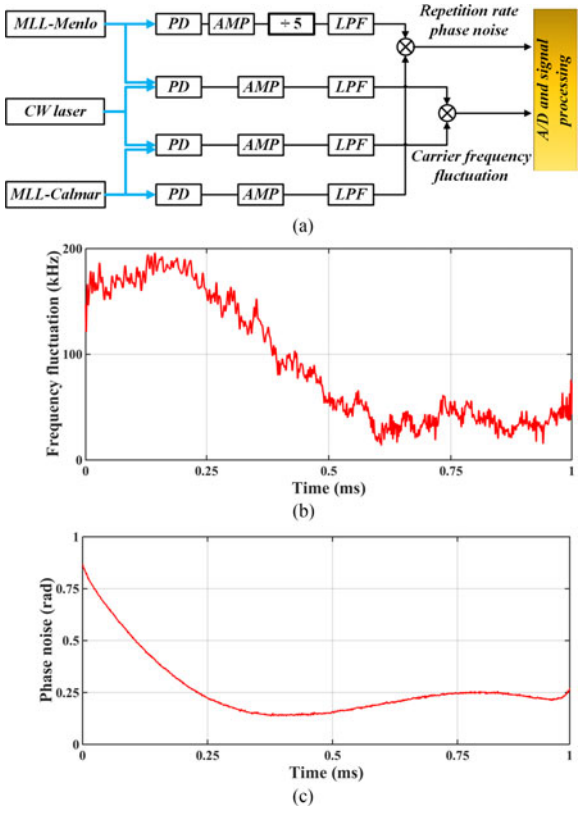

Fig. 6. (a) Experiment setup for carrier frequency fluctuation and repetition rate noise measurement. PD, photodetector; AMP, amplifier; LPF, low pass filter; (b) Measured carrier frequency fluctuations $d\phi_c(t)/dt$; (c) Measured repetition rate phase noise.

in Fig. 5(a) with red circle is caused by the carrier frequency noise. According to (6), the accuracy of signal intensity measurement is only determined by the stability of the repetition rates, so the slow phase fluctuations of the repetition rate do not affect the single shot reflected signal intensity profile measurement. But for a long measurement time with averages of multiple traces, the phase locking electronics [20] or phase compensation technique [21] are necessary to be adopted for a stable measurement.

6. Conclusion

In conclusion, we experimentally demonstrated an ultra-high-resolution OTDR system which uses ultrashort pulses as the optical sources and is coherently detected with the LOS technique. Experiments are carried out and the spatial resolution is characterized at the end facet reflection. In the experiment we adopt a digital CD compensation at long distances then achieved a spatial resolution of 340 μm at 10 km. This technique shows a new application prospect for OTDR system in ultra-high resolution distributed applications such as OID for PONs or precisely locating the abnormal reflections in aircrafts.

References

[1] C.-Y. Chong and S. P. Kumar, "Sensor networks: evolution, opportunities, and challenges," *Proc. IEEE*, vol. 91, no. 8, pp. 1247–1256, Aug. 2003.
[2] Y. Koshikiya, N. Araki, C. Kito, and F. Ito, "Compact and large capacity identification device for uniquely addressing optical components," in *Proc. Nat. Fiber Opt. Eng. Conf.*, 2012, Paper JTh2A–69.

[3] K. Aoyama, K. Nakagawa, and T. Itoh, "Optical time domain reflectometry in a single-mode fiber," *IEEE J. Quantum Electron.*, vol. QE-17, no. 6, pp. 862–868, Jun. 1981.
[4] A. P. Vandevender and P. G. Kwiat, "High efficiency single photon detection via frequency up-conversion," *J. Modern Opt.*, vol. 51, no. 9, pp. 1433–1445, Jun./Jul. 2004.
[5] M. Legré, R. Thew, H. Zbinden, and N. Gisin, "High resolution optical time domain reflectometer based on 1.55 μm up-conversion photon-counting module," *Opt. Exp.*, vol. 15, no. 13, pp. 8237–8242, 2007.
[6] C. Schuck, W. H. P. Pernice, X. Ma, and H. X. Tang, "Optical time domain reflectometry with low noise waveguide-coupled superconducting nanowire single-photon detectors," *Appl. Phys. Lett.*, vol. 102, no. 5, 2013, Art. no. 191104.
[7] L. Herrera, G. Amaral, and J. P. von der Weid, "Ultra-high-resolution tunable PC-OTDR for PON monitoring in avionics," in *Proc Opt. Fiber Commun. Conf. Exhib.*, 2015, pp. 1–3.
[8] Q. Zhao *et al.*, "Photon-counting optical time-domain reflectometry with superconducting nanowire single-photon detectors," in *Proc. IEEE 14th Int. Superconductive Electron. Conf.*, Jul. 2013, pp. 1–3,.
[9] B. J. Soller, D. K. Gifford, M. S. Wolfe, and M. E. Froggatt, "High resolution optical frequency domain reflectometry for characterization of components and assemblies," *Opt. Exp.*, vol. 13, pp. 666–674, 2005.
[10] X. Fan, Y. Koshikiya, and F. Ito, "Phase-noise-compensated optical frequency domain reflectometry with measurement range beyond laser coherence length realized using concatenative reference method," *Opt. Lett.*, vol. 32, pp. 3227–3229, 2007.
[11] Q. Liu, X. Fan, and Z. He, "Time-gated digital optical frequency domain reflectometry with 1.6-m spatial resolution over entire 110-km range," *Opt. Exp.*, vol. 23, pp. 25 988–25 995, Oct. 2015.
[12] S. Wang, X. Fan, Q. Liu, and Z. He, "Distributed fiber-optic vibration sensing based on phase extraction from time-gated digital OFDR," *Opt. Exp.*, vol. 23, pp. 33 301–33 309, Dec. 2015.
[13] K. Okamoto and F. Ito, "Ultrafast measurement of optical DPSK signals using 1-symbol delayed dual-channel linear optical sampling," *IEEE Photon. Technol. Lett.*, vol. 20, no. 11, pp. 948–950, Jun. 2008.
[14] K. Okamoto and F. Ito, "Dual-channel linear optical sampling for simultaneously monitoring ultrafast intensity and phase modulation," *J. Lightw. Technol.*, vol. 27, no. 12, pp. 2169–2175, Jun. 2009.
[15] C. Dorrer, D. C. Kilper, H. R. Stuart, G. Raybon, and M. G. Raymer, "Linear optical sampling," *IEEE Photon. Technol. Lett.*, vol. 15, no. 12, pp. 1746–1748, Dec. 2003.
[16] S. Wang, X. Fan, Q. Liu, and Z. He, "Ultra-high-resolution OTDR based on linear optical sampling with digital dispersion compensation," in *Proc. Asia-Pac. Opt. Sensors*, 2016, Paper Th3A.5.
[17] D. Derickson, *Fiber Optic—Test and Measurement*, 1st ed. Englewood Cliffs, NJ, USA: Prentice-Hall, 1998.
[18] A. Yariv, D. Fekete, and D. M. Pepper, "Compensation for channel dispersion by nonlinear optical phase conjugation," *Opt. Lett.*, vol. 4, pp. 52–54, 1979.
[19] G. Goldfarb and G. Li, "Chromatic dispersion compensation using digital IIR filtering with coherent detection," *IEEE Photon. Technol. Lett.*, vol. 19, no. 13, pp. 969–971, Jul. 2007.
[20] Y. Kim and Y. Dae-Su, "High-speed terahertz time-domain spectroscopy based on electronically controlled optical sampling," *Opt. Lett.*, vol. 35, pp. 3715–3717, 2010.
[21] T. Ideguchi, A. Poisson, G. Guelachvili, T. W. Hänsch, and N. Picqué1, "Adaptive dual-comb spectroscopy in the green region," *Opt. Lett.*, vol. 37, pp. 4847–4849, 2012.